

Systematical study of the optical potential for systems like $A + {}^{58}\text{Ni}$ from sub-barrier data analyses

L. R. Gasques,¹ L. C. Chamon,¹ D. Pereira,¹ M. A. G. Alvarez,¹ E. S. Rossi, Jr.,¹ C. P. Silva,¹ G. P. A. Nobre,¹ and B. V. Carlson²

¹*Departamento de Física Nuclear, Instituto de Física da Universidade de São Paulo, Caixa Postal 66318, 05315-970 São Paulo, São Paulo, Brazil*

²*Departamento de Física, Instituto Tecnológico de Aeronáutica, Centro Técnico Aeroespacial, São José dos Campos, São Paulo, Brazil*

(Received 19 December 2002; published 20 June 2003)

Elastic scattering differential cross sections were measured for the ${}^{28}\text{Si} + {}^{58}\text{Ni}$ system at sub-barrier energies. The corresponding nuclear potential was compared with earlier results of systems like $A + {}^{58}\text{Ni}$. The present data also allowed the determination of the ${}^{28}\text{Si}$ nuclear density through an unfolding method. The experimentally extracted ${}^{28}\text{Si}$ density values are compared with those previously obtained for the ${}^4\text{He}$, ${}^{12}\text{C}$, ${}^{16,18}\text{O}$ nuclei. We present a critical discussion of the absolute precision obtained for the density parameters extracted from the data analyses.

DOI: 10.1103/PhysRevC.67.067603

PACS number(s): 24.10.Ht, 21.10.Ft, 21.10.Gv

We present elastic scattering angular distributions for the ${}^{28}\text{Si} + {}^{58}\text{Ni}$ system at sub-barrier energies. One of the purposes of the experiment was the determination of the nuclear potential for this system in the surface region. This method was successfully applied to several other systems involving the same target and the ${}^{12}\text{C}$, ${}^{16,18}\text{O}$ nuclei as projectiles [1–6]. As discussed in these earlier works, at sub-barrier energies the imaginary part of the optical potential is negligible since the corresponding reaction cross section is very small. Therefore, the elastic scattering data analysis in this energy region unambiguously determines the real part of the interaction.

In recent works [7–10], we have developed a nonlocal model for the nuclear interaction that is based on quantum effects related to the exchange of nucleons between the target and projectile. The nonlocal model has provided a good description of the elastic and inelastic scattering, transfer, and fusion processes for several systems in a wide energy range [3,5,6,8–11]. The model has also provided good predictions for an extensive systematics of potential strengths extracted from heavy-ion elastic scattering data analyses [7]. In the present work, we compare the potential for the ${}^{28}\text{Si} + {}^{58}\text{Ni}$ system with the results of such a systematics and also with other results for systems involving the same target nucleus, i.e., ${}^{12}\text{C}$, ${}^{16,18}\text{O} + {}^{58}\text{Ni}$ (from Refs. [3,5,6]), and ${}^4\text{He} + {}^{58}\text{Ni}$ (the data for these systems can be found in Ref. [13], but the corresponding nuclear potentials were not published so far).

If the nonlocal model is assumed for the interaction and the density of one nucleus is known, an unfolding method can be used to extract the nuclear density of the other nucleus from the elastic scattering data analyses. The method has already been successfully applied in the experimental determination of densities for the ${}^4\text{He}$, ${}^{12}\text{C}$, and ${}^{16,18}\text{O}$ nuclei [5,6,12,13]. In the present work, we use this method in the data analyses of the ${}^{28}\text{Si} + {}^{58}\text{Ni}$ system at sub-barrier energies, with the aim of obtaining the ${}^{28}\text{Si}$ nuclear density in the surface region. We compare the ${}^{28}\text{Si}$ extracted density values with those experimentally obtained for the other nu-

clei. In this work, we also discuss the absolute precision for the experimentally extracted density parameters and the consistency of the results with an earlier extensive systematics of heavy-ion densities [7].

The measurements were made using the ${}^{28}\text{Si}$ beam from the São Paulo 8UD Pelletron Accelerator, Brazil. The detecting system was already described in Ref. [1]. Figure 1 shows the elastic scattering cross sections for the ${}^{28}\text{Si} + {}^{58}\text{Ni}$ system. In the optical model calculations, we have adopted a procedure similar to that described in the analyses of the sub-barrier data for several systems [1–6]. As a first step, we

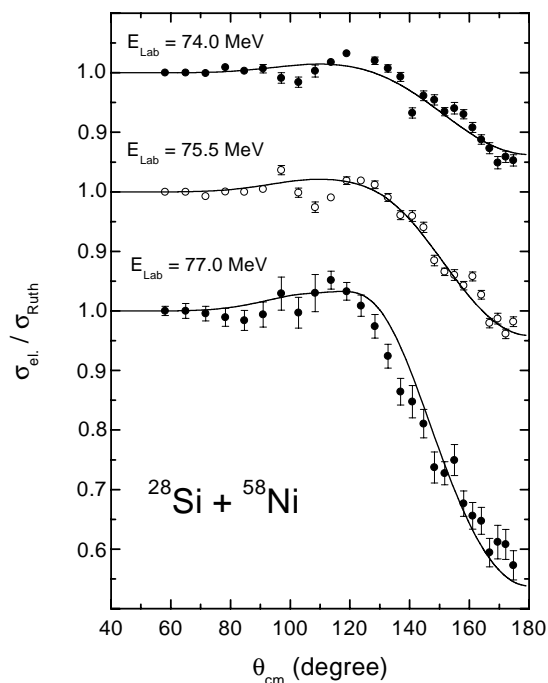


FIG. 1. Elastic scattering angular distributions for the ${}^{28}\text{Si} + {}^{58}\text{Ni}$ system at sub-barrier energies. The solid lines represent optical model predictions, in which the nonlocal model is assumed for the real part of the interaction.

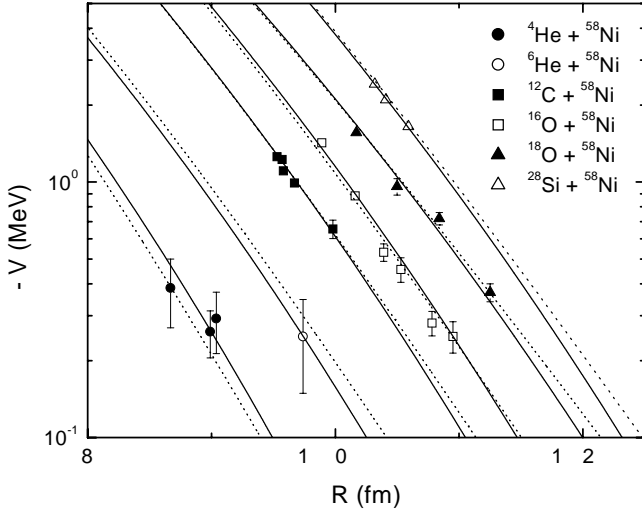


FIG. 2. The nuclear potential strength as a function of the sensitivity radius for the ${}^4\text{He}$, ${}^{12}\text{C}$, ${}^{16,18}\text{O}$, and ${}^{28}\text{Si} + {}^{58}\text{Ni}$ systems. The lines represent the results of the nonlocal model, using the matter distributions of the nuclei within the zero-range approach (solid lines) or the nucleon densities with the M3Y interaction (dashed lines). The parameters of the densities involved in the calculations are presented in Table I and Fig. 3.

have assumed a Woods-Saxon shape for the real and imaginary parts of the optical potential. Our experiments indicate that peripheral reaction channels present no significant cross section at the energy region in which the data were obtained. Taking this into account, the parameters of the imaginary part of the potential were taken so as to provide small strengths in the surface region and complete internal absorption from barrier penetration, through a large imaginary potential internal to the barrier and a regular boundary condition at the origin. With these conditions, the elastic scattering cross section predictions are quite insensitive to variations of the imaginary potential parameters. The depth and diffuseness parameters of the real part of the optical potential were searched for the best data fits. For each angular distribution, we found a family of potentials that give equivalent data fits. The point at which these potentials cross defines the sensitivity radius, where the value of the potential is determined without ambiguity (see, for example, Refs. [3–6]). At sub-barrier energies, the sensitivity radius is energy dependent and the nuclear potential can therefore be obtained over a large range of surface radial distances by varying the incident energy. This dependence determines the diffuseness of the potential, as can be observed in Fig. 2 for the ${}^4\text{He}$, ${}^{12}\text{C}$, ${}^{16,18}\text{O}$, ${}^{28}\text{Si} + {}^{58}\text{Ni}$ systems.

The elastic scattering data analyses for different systems in a wide energy range have resulted in phenomenological optical potentials with significant dependence on the bombarding energies [14]. We have developed a model that associates this dependence with nonlocal quantum effects [7–10]. Within this model, the bare interaction V_N is connected with the folding potential V_F through

$$V_N(R, E) \approx V_F(R) e^{-8[E - V_C(R) - V_N(R, E)]/\mu c^2}. \quad (1)$$

In the present work, the nonlocality correction has little effect since we analyze near barrier data. In this energy region the nonlocal potential is almost identical to the folding one [see Eq. (1)].

The folding potential depends on the densities of the two partners in the collision

$$V_F(R) = \int \rho_1(r_1) \rho_2(r_2) u_0(\vec{R} - \vec{r}_1 + \vec{r}_2) d\vec{r}_1 d\vec{r}_2. \quad (2)$$

In Ref. [7] a systematization of nuclear densities has been proposed, based on an extensive study involving experimental and theoretical densities. The two-parameter Fermi (2pF) distribution was adopted to describe the nuclear densities, and a distinction between nucleon and matter distributions was made by taking into account the finite size of the nucleon [7]. The radii of the 2pF distributions are well described by

$$R_0 = 1.31A^{1/3} - 0.84 \text{ fm}, \quad (3)$$

where A is the number of nucleons in the nucleus. The nucleon and matter densities present average diffuseness values of $\bar{a}_N = 0.50$ fm and $\bar{a}_M = 0.56$ fm, respectively. Owing to specific nuclear structure effects (single particle and/or collective), the parameters R_0 and a show small variations around the corresponding average values throughout the periodic table. However, as far as the folding potential is concerned, the effects of the structure of the nuclei are mostly present at the surface (of the potential) and are mainly related to the diffuseness parameter (of the densities) [7].

The extensive optical potential systematics of Ref. [7] was performed within this context. The experimental potential strengths were described within 25% precision, by combining Eqs. (1) and (2) through two different methods: (i) using the nucleon distributions of the nuclei and an appropriate form for the nucleon-nucleon interaction, and (ii) using the matter distributions of the nuclei with a zero-range approach for $u_0(\vec{r})$. As shown in Ref. [7], both alternatives are equivalent in describing the heavy-ion nuclear potential.

In Ref. [7], we also demonstrated that the folding potential arising from 2pF distributions with slightly different diffuseness parameters can be appropriately simulated by considering the folding of two distributions with the same diffuseness value: $a = (a_1 + a_2)/2$. This procedure was used in the present work to describe the experimental potential strengths (see the solid lines in Fig. 2). Equation (3) gives accurate results for the radii of heavy nuclei, but it fails in the case of light nuclei in which the effects of structure are more significant [7]. Therefore, for the ${}^4\text{He}$ we have also considered more realistic radii as obtained in Refs. [13,15] (see Table I). The values of the matter diffuseness were considered as free parameters and adjusted to reproduce the experimental potential strengths. The resulting values are presented in Table I. The results obtained with the nonlocal model for the elastic scattering cross sections of the ${}^{28}\text{Si} + {}^{58}\text{Ni}$ system are presented in Fig. 1 (solid lines). The theoretical calculations fail to reproduce the oscillations observed in the dataset. We believe that such oscillations are

TABLE I. The diffuseness values of the matter distributions and the radii of the projectiles considered in the calculations of the nuclear potentials.

System	Model	R_0 (fm)	a_M (fm)
$^4\text{He} + ^{58}\text{Ni}$	Eq. (3)	1.24	0.50
	Ref. [13]	1.64	0.48
	Ref. [15]	1.26	0.50
$^6\text{He} + ^{58}\text{Ni}$	Eq. (3)	1.54	0.54
	Ref. [15]	1.23	0.56
$^{12}\text{C} + ^{58}\text{Ni}$	Eq. (3)	2.16	0.56
$^{16}\text{O} + ^{58}\text{Ni}$	Eq. (3)	2.46	0.57
$^{18}\text{O} + ^{58}\text{Ni}$	Eq. (3)	2.59	0.61
$^{28}\text{Si} + ^{58}\text{Ni}$	Eq. (3)	3.14	0.58

due to the coupling to some particular reaction channel. However, we have not investigated this possibility in the present work, because our intent is to show the quality of the predictions of the nonlocal model. An inspection of Fig. 1 shows that such predictions are in agreement with the average behavior of the data.

The values for the matter diffuseness presented in Table I should be compared with the average diffuseness obtained in the extensive systematics of Ref. [7]: $\bar{a}_M = 0.56$ fm. In the systematics, a dispersion (standard deviation) of about 0.025 fm around the average value was found and was associated with effects of the structure of the nuclei throughout the periodic table. The $^4\text{He} + ^{58}\text{Ni}$ and $^{18}\text{O} + ^{58}\text{Ni}$ systems present matter diffuseness differing from the average value ($\bar{a}_M = 0.56$ fm) by about two standard deviations. In the ^{18}O case, this behavior is connected with the two off-shell valence neutrons [6]. On the other hand, from electron scattering experiments, the diffuseness of the ^4He charge distribution has already been found to be significantly smaller than those for heavy ions [16]. We mention that the large uncertainty of the potential strength for the $^6\text{He} + ^{58}\text{Ni}$ system (see Fig. 2) results in a large uncertainty (about 0.03 fm) for the corresponding density diffuseness.

If the nonlocal model is assumed for the interaction, and the density of one nucleus is known, an unfolding method can be used to extract the ground-state nuclear density of the other nucleus through the elastic scattering data analyses. Here, the double-folding potential is considered in the usual form: the nucleon densities and the M3Y effective nucleon-nucleon interaction are adopted in Eq. (2). The method has been successfully applied in the experimental determination of densities for the $^4,^6\text{He}$, ^{12}C , and $^{16,18}\text{O}$ nuclei, and the resulting densities have been shown to be consistent with the experimental electron scattering data [5,6,12,13]. In the present paper, we describe the method in a quite concise manner, and we invite the reader to obtain further details in a complete discussion presented in Refs. [5,6,12]. In the data analyses, we have used a theoretical Dirac-Hartree-Bogoliubov density for the ^{58}Ni nucleus [17], since the resulting predictions for electron scattering cross sections are in very good agreement with the data [5,12]. The ^{28}Si density was obtained with a procedure similar to that used in the

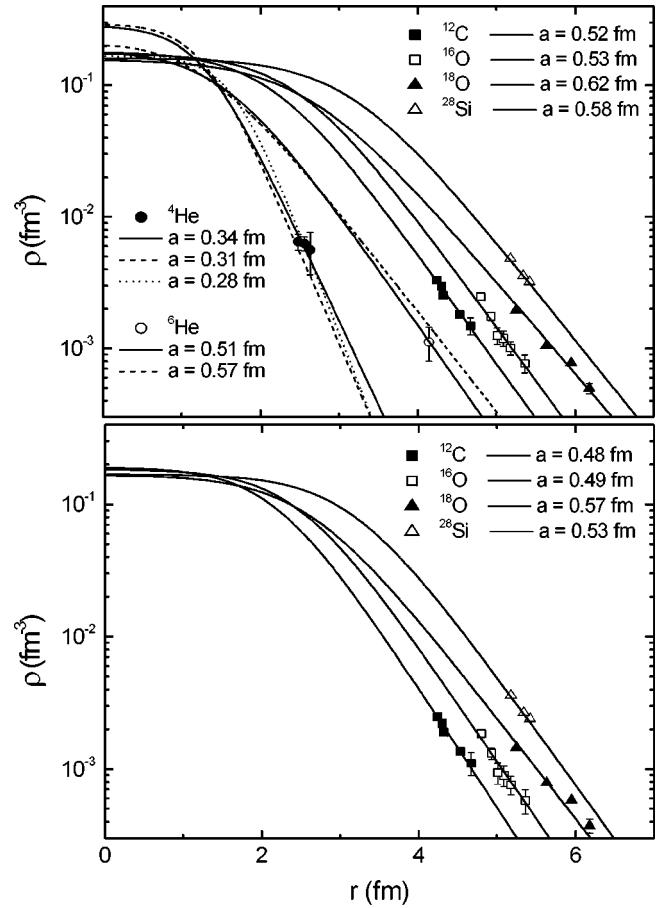


FIG. 3. Top—experimental nucleon density values at the sensitivity radii for the $^4,^6\text{He}$, ^{12}C , $^{16,18}\text{O}$, and ^{28}Si nuclei, extracted from elastic scattering data analyses at sub-barrier energies. The solid lines correspond to two-parameter Fermi distributions, with radii obtained from Eq. (3) (see Table I) and diffuseness values as indicated in the figure. The dashed and dotted lines correspond to realistic SF and 2pF distributions obtained in Refs. [15,13], respectively. Bottom—the density values have been decreased by 25%, and the corresponding diffuseness values have been recalculated.

determination of the potential strengths at the sensitivity radii. We have assumed the 2pF distribution to describe the ^{28}Si density. The diffuseness (a_N) and radius (R_0) were searched for the best elastic scattering data fits, with the ρ_0 parameter determined by the normalization condition. For each angular distribution, we have found a family of densities that give equivalent data fits. These densities cross at the sensitivity radius, where the value of the density is determined without ambiguity.

Figure 3 (top) contains the experimental nucleon density values for $^4,^6\text{He}$, ^{12}C , $^{16,18}\text{O}$, and ^{28}Si at the corresponding sensitivity radii, as obtained from elastic scattering data analyses of several angular distributions for $A + ^{58}\text{Ni}$ systems. The statistical error bars for the density values have been determined as described in Ref. [5]. We have adjusted 2pF distributions to the experimental density values (solid lines in Fig. 3, top), using the corresponding radii of Eq. (3) (see Table I) and considering the nucleon diffuseness as a free parameter. The results obtained for the values of the

diffuseness are indicated in Fig. 3 (top). The dashed lines in Fig. 2 represent the nuclear potentials obtained using these 2pF distributions for the nucleon densities of the projectiles and the M3Y effective nucleon-nucleon interaction.

As demonstrated earlier [5,6,12,13], information about the density in the surface region is obtained from sub-barrier elastic scattering data analyses, while intermediate energy data analyses probe the density in much inner distances. This fact has already been used [13] to determine a 2pF distribution for the ${}^4\text{He}$ nucleus (dotted line in Fig. 3, top). The corresponding results for the radius and diffuseness are indicated in Table I and Fig. 3 (top), respectively. In Ref. [15], the nuclear ${}^{4,6}\text{He}$ densities were obtained from elastic scattering data analyses for the ${}^{4,6}\text{He}+p$ systems at 700 MeV/nucleon, using the Glauber multiple scattering theory for the interaction. In that work, different parametrizations for the ${}^6\text{He}$ density were tested, including symmetrized Fermi (SF) distributions. For the purpose of comparison, the corresponding SF distributions for the ${}^{4,6}\text{He}$ nuclei are included as dashed lines in Fig. 3 (top), and the corresponding radii and diffuseness are presented in Table I and Fig. 3 (top).

The values found in the present work for the nucleon diffuseness of the ${}^{12}\text{C}$, ${}^{16,18}\text{O}$, and ${}^{28}\text{Si}$ nuclei are somewhat greater than the average value ($\bar{a}_N=0.50$ fm) obtained in the systematics of Ref. [7]. This seems to be an inconsistent result. However, the determination of density values at the sensitivity radii is exposed to systematical errors that arise from several sources: (i) the dependence of the results on the shape assumed for the projectile; (ii) the theoretical density assumed for the target; (iii) the contribution of the polarization potential that has not been included in our analyses, etc. In previous works [5,6,12,13], we have estimated the systematical error of the density values as 20% to 30%. With the aim of illustrating the effect of this error in the determination of the diffuseness of the density distributions, in Fig. 3 (bottom) we show experimental density values decreased by 25% in comparison with those of Fig. 3 (top). The corre-

sponding values of the diffuseness are about 7% smaller than those obtained without the reduction (see Fig. 3), and they approach the average diffuseness obtained in Ref. [7].

In this work, we have presented elastic scattering data at sub-barrier energies for the ${}^{28}\text{Si}+{}^{58}\text{Ni}$ system. The corresponding data extracted nuclear potentials at the sensitivity radii have been compared with those for the ${}^{4,6}\text{He}$, ${}^{12}\text{C}$, and ${}^{16,18}\text{O}+{}^{58}\text{Ni}$ systems. All the results for the potentials are in very good agreement with the nonlocal model in the context of the systematics for the nuclear densities of Ref. [7]. We have also applied the nonlocal model to extract density values from data analyses. In this case, larger systematical errors are expected in comparison with those involved in the determination of potential strengths. Within the estimate of the systematical uncertainties, the density diffuseness experimentally extracted from data analyses is also in good agreement with the systematics of Ref. [7]. The uncertainty of the absolute values for the diffuseness is about 7%, but the comparison of results for different nuclei is probably less exposed to systematical errors. In fact, the use of the same method (and same target nucleus) would provide partial cancellation of the effects of the systematical errors. Taking this into account, our results clearly demonstrate that the ${}^4\text{He}$ and ${}^{18}\text{O}$ have, respectively, the smallest and the greatest diffuseness among all the nuclei studied in the present work. The ${}^{12}\text{C}$, ${}^{16}\text{O}$, and ${}^{28}\text{Si}$ nuclei present similar diffuseness approaching the average value of Ref. [7]. Besides the systematical error, the diffuseness of the ${}^6\text{He}$ exotic nucleus has been determined within greater statistical uncertainty (≈ 0.03 fm), but our analysis indicates that its diffuseness is comparable with those of heavy nuclei and much greater than the value found for the neighboring stable ${}^4\text{He}$.

This work was partially supported by Fundação de Amparo à Pesquisa do Estado de São Paulo (FAPESP) and Conselho Nacional de Desenvolvimento Científico e Tecnológico (CNPq).

-
- [1] L.C. Chamon *et al.*, Nucl. Phys. **A582**, 305 (1995).
 - [2] L.C. Chamon *et al.*, Nucl. Phys. **A597**, 253 (1996).
 - [3] M.A.G. Alvarez *et al.*, Nucl. Phys. **A656**, 187 (1999).
 - [4] C.P. Silva *et al.*, Nucl. Phys. **A679**, 287 (2001).
 - [5] L.R. Gasques *et al.*, Phys. Rev. C **65**, 044314 (2002).
 - [6] E.S. Rossi, Jr., *et al.*, Nucl. Phys. **A707**, 325 (2002).
 - [7] L.C. Chamon *et al.*, Phys. Rev. C **66**, 014610 (2002).
 - [8] M.A. Cândido Ribeiro *et al.*, Phys. Rev. Lett. **78**, 3270 (1997).
 - [9] L.C. Chamon *et al.*, Phys. Rev. Lett. **79**, 5218 (1997).
 - [10] L.C. Chamon *et al.*, Phys. Rev. C **58**, 576 (1998).
 - [11] L. R. Gasques *et al.* (unpublished).
 - [12] M.A.G. Alvarez *et al.*, Phys. Rev. C **65**, 014602 (2002).
 - [13] L.R. Gasques *et al.*, Phys. Rev. C **67**, 024602 (2003).
 - [14] M.E. Brandan and G.R. Satchler, Phys. Rep. **285**, 142 (1992), and references therein.
 - [15] G.D. Alkhazov *et al.*, Phys. Rev. Lett. **78**, 2313 (1997).
 - [16] H. De Vries, C.W. De Jager, and C. De Vries, At. Data Nucl. Data Tables **36**, 495 (1987).
 - [17] B.V. Carlson and D. Hirata, Phys. Rev. C **62**, 054310 (2000).